A study on giant radio pulses

Karuppusamy, R.

CHAPTER 6

Giant pulses from Millisecond Pulsars

Abstract This chapter presents the results of a search for giant pulses from a selection of millisecond pulsars. Utilising the flexibility of a baseband recording based pulsar machine like PuMa-II we were able to use the high precision pulsar timing data for this search. We detected giant pulses from PSR B1937+21 but failed to detect them from PSRs B1821−24, J0218+4232 and B1957+20. In all three cases the lack of detection was consistent with previous determinations of giant pulse strengths and emission rates. We discuss an improved technique for searching the PuMa II data for giant pulses which has already resulted in many more detection from PSR B1937+21. We plan to make GP searches part of the standard processing pipeline for all MSP observations in the future.

6.1 Introduction

In this chapter, the results of a study of giant pulses from millisecond pulsars is presented. The weak nature of the individual pulses from millisecond pulsars (MSPs) makes them difficult to detect. However, bright narrow radio emission from MSPs are known to occur and provided a sensitive system, these pulses could be detected. The phenomenon of giant pulses was reported for the first time from the Crab pulsar (Argyle & Gower 1972) and are defined as the pulses with energy greater than ten times the average pulse energy and tend to be much narrower than the average emission from the pulsar. The second source of giant pulses was PSR B1937+21 (Cognard et al. 1996) and in this pulsar these pulses were found to be occur in narrow pulse phases trailing the average emission profile. Following this report, Kinkhabwala & Thorsett (2000) carried out an extensive multifrequency study of B1937+21 giant pulses to determine the emission rates and Soglasnov et al. (2004) found that these pulses can be as narrow as 15 ns. The next candidate that showed giant pulse emission was the MSP PSR B1821−24 (Romani & Johnston 2001), followed by PSRs J0218+4232, J1823-3021A and B1957+20(Knight et al. 2006b, 2005). In the Crab pulsar, the emission from giants modulate the whole phase range of the average pulse profile (for an alternate interpretation, see Chapter 5 and Popov et al. 2006a), while in the MSPs they always occur in narrow pulse phases separate from the average emission. Another young pulsar in the Large Magellenic Cloud, PSR B0540-69 was reported to show emission of these anomalous pulses (Johnston & Romani 2003) and the pulses show characteristics similar to those from the Crab pulsar. The only common factors in the pulsars mentioned above are their high energy emission, and large ($B_{LC} \approx 10^5$ G) magnetic field at the velocity of light cylinder.

As noted by Romani & Johnston (2001), giant pulses from PSR B1821-24 shows a remarkable phase coincidence with the high energy pulsed emission and this was confirmed later in two more MSPs. For example, the giant pulses from PSR B1937+21 coincide with phase of the non-thermal X-Ray emission (Cusumano et al. 2003). The same behaviour was noted in PSR J0128+4232 (Knight et al. 2006b). This suggests that the giant pulse and high-energy emission regions are co-located in the pulsar magnetosphere. Therefore, in addition to large B_{LC}, the presence of pulsed high energy emission appears to be correlated to the radio giant pulses in a pulsar.

In contrast to the above, recently giant pulse like emission was found in pulsars with apparently low B_{LC} ∼4–100 G and no high energy counterparts. These pulsars are dealt with in Chapter 4. These contrasting observations shows that the radio emission from pulsars is not a very well understood phenomena. The large amount of energy in the single giant pulses and the association with high energy emission means that the emission process that generates them is important and interesting. Moreover as indicated by (Petrova 2004), there is a possible association with the lower energy emission as well. It is also interesting to note that the result of Shearer et al. (2003), who showed that the correlation with the coherent and incoherent emission processes may provide us with a further constraint on the properties of the plasma in the magnetosphere. Therefore, additional observational information on the giant pulses can possibly uncover the nature of the radio emission mechanism.

Observationally, the giant pulses are seen as bright bursts and differ from the normal

pulsed emission in terms of their energy and flux distributions. The common characteristics of the giant pulses from the pulsars mentioned above are that the pulse energy and flux distribution exhibit a power law nature (e.g Lundgren et al. 1995; Kinkhabwala & Thorsett 2000), quite distinct from the gaussian distribution of the normal pulses (Hesse & Wielebinski 1974). Past studies on the giant pulses from MSPs were based on ~200 giant pulses except in PSR B1937+21. Additional data can be used to characterize these pulses extensively. The results described in this chapter are derived from a second pass processing of pulsar timing observations, which is carried out every month. Therefore, this method potentially allows one to access a large population of giant pulses.

The rest of the chapter is organised as follows: the details of the observation and data reduction are presented in §6.2, followed by the system sensitivity considerations in §6.3. The giant pulses detected from PSR B1937+21 is presented next, followed by discussion and conclusion.

6.2 Observations and data reduction

The data used here are from several observations carried out in 2007–2009, primarily acquired as a part of the long running Pulsar Timing programme at the Westerbork Synthesis Radio Telescope (WSRT). The observational details are displayed in Table 6.1. As discussed in the previous chapters, voltages from the single telescopes are sampled at 2-bit resolution and a rate of 40 MHz. These are written as 8-bit baseband data after the coherent addition of 2-bit data from the individual telescopes.

The baseband data is then processed using the open-source package DSPSR. All four polarization products were formed using an 8-channel coherent synthetic filterbank and the data was written to disk as single pulses. This frequency resolution permitted 1024 or 2048 phase bins across the pulse period of the pulsars studied here. The total intensity of the pulses were then computed and searched for giant pulse emission. We chose a criteria of S/N =7–9 σ, where S/N is the signal-to-noise ratio and σ is the offpulse root-mean-square fluctuation. The design of the WSRT and PuMa-II results in up to eight 10 or 20 MHz bands at each observation frequency. The giant pulse search was performed independently in every recorded band.

6.3 Sensitivity to giant pulses

Below we summarize the giant pulse detections using two methods. In the first method, giant pulses were detected in each individual 20/10 MHz subbands. Pulses that satisfy the threshold criteria were retained for further analysis and the rest deleted. In the second method, single pulses were first formed in all subbands. These pulses were then added across the frequency bands in software resulting in pulses with an equivalent bandwidth of either 80 or 160 MHz, depending on the sky frequency of the observation. The pulses with larger bandwidth resulted in a lower radiometer noise and were then searched for giant pulses. This

Pulsar	Date	Band [a,b,c]	Duration
	dd-mm-yyyy		minutes
B1937+21	03-02-2007	21cm	11
	11-02-2007	21cm	21
	25-02-2007	21cm	15
	24-03-2008	21cm	20
	24-05-2008	13cm	20
	22-06-2008	21cm	20
	22-06-2008	13cm	20
	20-06-2009	21cm	35
	20-06-2009	13cm	35
B1821−24	04-02-2007	21cm	25
	25-02-2007	21cm	20
	24-06-2007	21cm	26
	29-03-2008	21cm	25
	24-04-2008	21cm	35
	22-06-2008	21cm	35
	08-10-2008	21cm	35
	26-05-2009	21cm	29
	20-06-2009	21cm	25
J0218+4232	24-05-2008	21cm	26
	19-07-2008	21cm	25
	26-05-2009	92cm	25
	26-05-2009	21cm	25
	20-06-2009	21cm	25
	20-06-2009	92cm	25
B1957+20	24-05-2008	92cm	30

[a] 92cm band refers to eight 10 MHz bands at 376.25, 367.5, 358.75, 350, 341.25, 332.5, 323.75 and 315 MHz.

[b] 21cm band refers to eight 20 MHz bands at 1310, 1330, 1350, 1370, 1390, 1410, 1430 and 1450.

[c] 13cm band refers to eight 20 MHz bands at 2210, 2228.125, 2246.25, 2264.375, 2282.5, 2300.625, 2318.75 and 2336.875

Table 6.1: Observational details for the millisecond pulsars considered in this study. The last column is the duration of the observation in minutes.

method was employed only for the observations done on 20/21–06–2009, since the software to combine pulses is a new development.

6.3.1 20/10 MHz subband detections

The system sensitivity to the giant pulses from the MSPs observed in the three different bands at the WSRT are listed in Table 6.2. The minimum detectable signal is computed using the expression 4.1. The relevant parameters are $B = 20$ MHz, and T_{int} are listed in column 4 of Table 6.2. The telescope gains were taken from the the WSRT user's manual [1]. The system temperature, $T_{sys} = T_{rx}+T_{sky}$, where T_{rx} is the receiver temperature. The sky temperature T_{sys} is computed assuming that the synchrotron contribution from the Galactic background scales with frequency as $\nu^{-2.6}$ and using the nominal sky temperature from 408 MHz continuum maps of Haslam et al. (1981).

Pulsar	Band	T_{sys} (K)	T_{int} (μs)	S_{min} (Jy)
B1957+20.....	92cm	204	0.78	347
B1937+21.....	21cm (13cm)	33 (61)	0.76	63 (115)
B1821−24.....	21cm	35	2.98	33
J0218+4232.....	92cm (21cm)	185 (31)	1.13	295 (48)

Table 6.2: Telescope sensitivity to various pulsars. Observation parameters of pulsars at two different frequencies are shown in parentheses. The frequencies considered for 92cm, 21cm and 13cm band are 328, 1400 and 2273 MHz, respectively. At 92cm a bandwidth of 10 MHz is considered, and it is 20 MHz at the other two frequencies. The factor S_{min} corresponds to the 8σ detection threshold.

In these observations, we have detected 25 giant pulses from PSR B1937+21 in the 1300–1460 MHz band. No single pulses were detected from this pulsar in the 2200–2360 MHz band. From Table 6.2, we can see that the large system temperature in this frequency band resulted in a lower sensitivity. Moreover, at 2.2 GHz the giant pulse emission rates is also lower than at 1400 MHz (Kinkhabwala & Thorsett 2000). These two factors resulted in no giant pulse detections.

From our observations of PSR B1821−24 and J0218+4232 , we did not detect any single pulse with $S/N \geq 7\sigma$. Therefore, we now derive the emission rate of the giant pulses in these pulsars and compare with the previous studies. The probability of detecting a giant pulse above our detection threshold in at least one of the observing sessions is given by,

$$p = \sum_{i=1}^{N} \frac{1}{t_i/P} \tag{6.1}$$

where, t_i is the time in seconds of the observing session i and P is the pulse period in seconds. Using the values of t_i from Table 6.1, the upper limit of probability of detecting a pulse with

[1] http://www.astron.nl/radio-observatory/astronomers/wsrt-guide-observations/

peak intensity $S_{peak} > 33$ Jy is $p = 1.67 \times 10^{-5}$. True emission rates may be less than than this value.

To compare with the previously published giant pulse emission rates, we convert our values in terms of the mean pulse energy $\langle E \rangle$. In the 21cm band, PSR B1821−24 has a mean flux of 0.18 mJy [2] (Hobbs et al. 2004). Therefore in our observations a $\sim 3\mu$s wide pulse with a peak intensity of 33 Jy corresponds to a pulse energy of $183\langle E \rangle$. Knight et al. (2006a) derive an expression for the probability of occurrence of a pulse with energy $E > E_0$ as $K.E_0^{-1.6}$, where E_0 is expressed in terms of $\langle E \rangle$ and $K = 2.5 \times 10^{-4}$. These authors also find a rate of 1.3×10^{-5} for pulses $\geq 28\langle E \rangle$. With their value of K, we compute the rate of a pulse with $183\langle E \rangle$ as 6×10^{-8}. The value we derive here is an upper limit, and therefore consistent with Knight et al. (2006a).

Proceeding in a manner similar to the above, we derive the giant pulse emission probability for PSR J0218+4232 and these values are 6.1×10^{-6} and 3×10^{-6} for 21cm and 92cm observations, respectively. At 21cm we were sensitive to pulses greater than 48 Jy peak flux corresponding to a pulse energy of ∼55 Jy.μs. Referring to the ATNF pulsar catalogue, the mean flux density of this pulsar at 1400 MHz is 0.9 mJy. So, our threshold in mean pulse energy is $32\langle E \rangle$. This is consistent with the rate of 3.8×10^{-7} derived by Knight et al. (2006b) for pulses with energy greater than $20\langle E \rangle$.

6.3.2 160/80 MHz detections

Pulsar	Band	T_{sys} (K)	T_{int} (μs)	S_{min} (Jy)
B1937+21.....	21cm (13cm)	33 (61)	0.76	16 (29)
B1821−24.....	21cm	35	2.98	8
J0218+4232.....	92cm (21cm)	185 (31)	1.13	104 (12)

Table 6.3: Telescope sensitivity to various pulsars - similar to Table 6.2, but the bandwidth is 160 MHz at 21/13cm and 80 MHz at 92cm. This refers to observations carried out on 20-06-2009. The factor S_{min} is the 8σ detection threshold.

The method described here is only in use since June 2009, but the effectiveness is evident from the results presented in the next section. As in §6.3.1, the 8-channel coherently dedispersed pulsar signal in each band was first written as single pulses to disk. Common pulses in the eight bands were identified based on the dispersion delay and then combined in software. An example is displayed in Figure 6.1. The resulting pulses have an equivalent bandwidth of 160 MHz, but a time resolution dictated by the number of channels used in each 20 MHz band. The resulting time resolutions and sensitivities are listed in Table 6.3.

From PSR B1937+21, a total of 53 pulses were detected at 21cm using a bandwidth of 160 MHz. These pulses are shown in Figure 6.2 and are discussed in the next section. For the higher frequency observations at 13cm, referring to Figure 9 of Kinkhabwala & Thorsett

[2] obtained from http://www.atnf.csiro.au/research/pulsar/psrcat

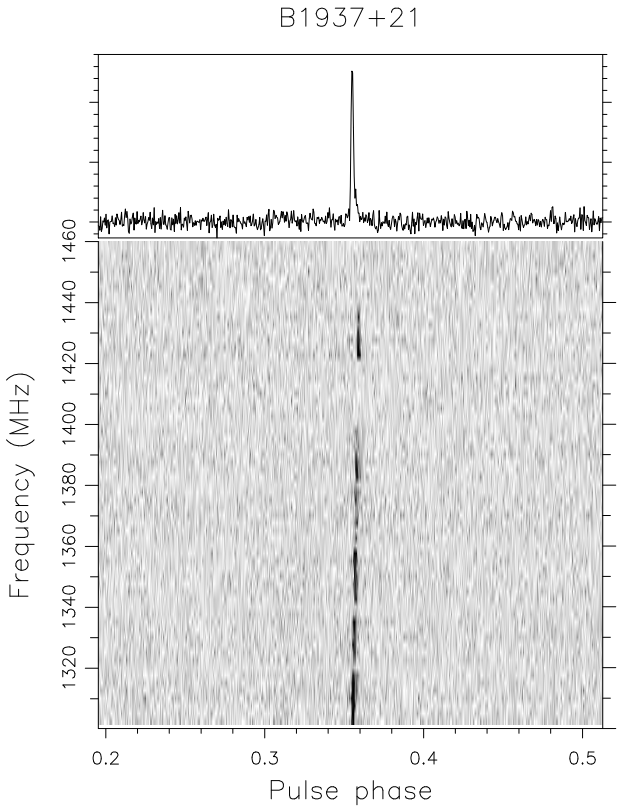

Figure 6.1: An example of a narrow bright pulse from the PSR B1937+21 detected in most bands. The top panel shows the total intensity of the pulse after combining the signal in all eight bands.

(2000), only a single pulse with peak intensity ≥ 30 Jy in 26 minutes is expected. Therefore, it is not surprising no giant pulses are detected in our 13cm observation.

Our analysis showed no giant pulses from the other MSPs, despite the improved sensitivity brought about by combining multiple subbands. Therefore, we proceed as in §6.3.1 to derive the giant pulse emission rates with the improved sensitivity. From the 25-minute observation of PSR B1821−24, the probablity of detecting a giant pulse with energy greater than $44\langle E\rangle$ is less than 2×10^{-6}. Since the value here is an upper limit, it is consistent with the rate of 5.8×10^{-7} derived from expression 1 of Knight et al. (2006a).

Similarly for PSR J0218+4232, the occurrence rates are less than 1.5×10^{-6} for pulses with energies greater than $1.5\langle E\rangle$ and $7\langle E\rangle$ for our 92cm and 21cm observations, respectively. In the case of PSR B1957+20, Knight et al. (2006b) detected a few bright pulses with energies in the range 4.5–8.6 $\langle E\rangle$. However, these are not considered giant pulses, because they do not seem to possess other characteristics shared by the giant pulses in milliseconds pulsars. The rate derived in their work is 5×10^{-8}, which is too small for any of the bright pulses to be

detected in our observations.

The giant pulse search was carried out using a procedure that is common to all pulsars considered here. The detection of giant pulses only in B1937+21 confirms that the method is robust and the non-detection of giant pulses in other pulsars is due to the comparatively smaller observation times that limits sensitivity to giant pulses. Two factors may have impacted our ability to detect giant pulses: possible errors in the value of dispersion measures (DM) of the pulsars and inadequate time resolution. In the 1400–2200 MHz range, pulses from PSR B1937+21 on the order of 10–100ns (Popov & Stappers 2003). This implies that our coarse time resolution of 760 ns time resolution can potentially reduce the S/N of a 100ns giant pulses by a factor of $\sim \sqrt{7.6}$. This effect is even more severe in the 13cm observations of PSR B1937+21.

For PSRs B1821-24 and J0218+4232, the giant pulses are of the order of 1.1 μs at 1700 MHz and 500 ns at 1373 MHz (Knight et al. 2006a,b). Assuming that scintillation in the interstellar medium broadens the pulses and follows a $\nu^{-4.4}$ scaling law, giant pulses from PSR B1821-24 are expected to be 2.75 μs at 1380 MHz, and therefore with our time resolution, the giant pulses were not under resolved. In the case of 328 MHz observations of PSR J0218+4232, the scaling law used above gives a pulse broadening time of 272 μs, thereby comfirming that our time resolution was adequate.

The extent of pulse smearing by the use of an inaccurate DM is considered next. At 1400 MHz, the DM of PSR B1937+21 should be better than 71.037±0.0015 to result in smearing error less than our final resolution of 0.76μs. Similarly, for PSRs B1821-24 and J0218+4232 the accuracy in the DM has to be better than 119.8289±0.00436 and 61.250±0.0022, respectively.

6.4 Giant pulses from B1937+21

From our observations, we detected a total of 78 giant pulses from B1937+21. All giant pulses detected are shown in Figure 6.2. As noted by Kinkhabwala & Thorsett (2000), the giant pulses trail the average emission phase. For the main pulse, the giants appear 0.035 later in phase than the peak emission phase and it is 0.041 for the inter pulse phase. These values are comparable to the phase differences of 0.036 and 0.045 for the main and interpulse giants as shown in Figures 2 & 3 in the former work.

Significant scintillation was present in the observations of PSR B1937+21, and as seen in Figure 6.1. In the frequency phase plane, the pulsar signal is absent in bands centred at 1410 and 1450 MHz, which is due to diffractive interstellar scintillation. This effect is discussed in detail for the case of Crab pulsar in Chapter 3. Similar analysis can be done to derive the scintillation bandwidth and time scales.

At the time of writing this report, a new software module is being developed, which shall allow one to combine the signal from the eight bands and then coherently dedisperse. This will improve the time resolution by a factor of 8 because $\Delta t = 1/B$, where B is bandwidth and is equal to 160 MHz. Therefore, we will be able to acheive a time resolution of 3.6ns. This aids giant pulse studies greatly because pulses from B1937+21 are found to be as narrow as 15 ns as reported by Soglasnov et al. (2004).

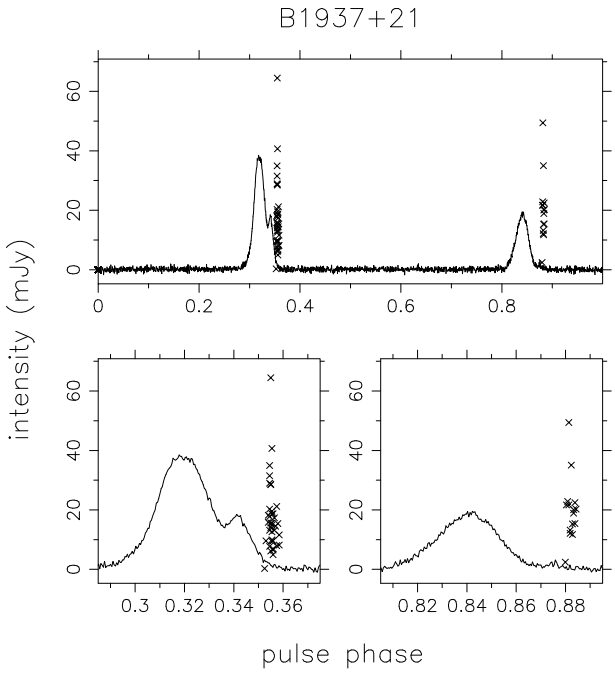

Figure 6.2: Narrow bright pulses from the PSR B1937+21. Relevant sections of the top panel are zoomed in the lower panels.

6.5 Discussion and conclusion

The results reported in this chapter shows an example of the effectiveness of giant pulse studies from MSPs using data obtained for a totally different purpose. The flexiblity and the high time resolution offered by the PuMa-II instrument (Chapter 2) have been crucial for the success of this method as evidenced from giant pulse detections in PSR B1937+21. The new technique of combining single pulses from the subbands has almost doubled the number of detections in a single observing session. Similarly, if the software to synthesise the 160 MHz signal from the 8×20 MHz signals is perfected, the number of giant pulses detected can increase even further as this avoids certain software issues in the distributed computing environment of PuMa-II.

The MSPs considered in this study show typically large dispersion measures (DMs) and small pulse periods. A very high accuracy in the DMs is required to be sensitive to the narrow giant pulses. Therefore, the future giant pulse search software needs be made sensitive to the small changes in DMs.

It is known that the signal from these pulsars have significant propagation effects seen as interstellar scintillation. Such scintillation affects the giantpulses and the average pulse identically. The average profiles in some of the observations show large intensity variations in the

160 MHz band. Knight et al. (2006a) further find that the diffractive scintillation parameters as $\Delta\nu_d \sim 0.1$ MHz and $\Delta t_d \sim 100$s at 1400 MHz in the direction of PSR B1821−24. Both of the parameters are sufficiently small as to not affect our observations significantly. In addition to the smaller rates of emission, the non-detections may be due to an unfavourable refractive interstellar scintillation in our observations. This argument is also valid for PSR J0218+4232. If the timing observations from these pulsars are searched with the new technique of combining the subbands, we should be able to uncover many of the giant pulses from these two pulsars, and hence characterize them robustly. The high resolution studies awaits further software development and that would allow us to routinely examine giant pulse emission much more effectively.

The γ-ray pulsations from PSR J0218+4232 (Kuiper et al. 2000) has a phase coincidence with its non-thermal X-ray emission (Kuiper et al. 2002). Moreover Knight et al. (2006b) find a phase correlation between the giant pulse and the X-ray emissions in this pulsar. Therefore, if the non-thermal γ-ray emission is an indicator of the presence of radio giant pulses then the discovery of γ-ray emission in PSRs J0030+0451, J0751+1807 and J1614-2230 by the Fermi consortium (Abdo et al. 2009b) opens up a possiblity of finding new MSP sources of giant pulses. The forthcomming results from the Fermi observations might reveal more sources of γ-ray pulsations from radio pulsars, providing additional candidates for the future searchs.

6.6 Acknowledgements

We acknowledge the use of European Pulsar Data network, the ATNF pulsar catalogue and the SAO/NASA Astronomical Data System maintained by Harvard-Smithsonian Center for Astrophysics. The WSRT is operated by ASTRON/NWO. We thank the observers for the setting up the telescope system prior to the observations. The PuMa-II instrument and RK are funded by Nederlands Onderzoekschool Voor Astronomie (NOVA).